JOURNAL OF MATERIALS SCIENCE 19 (1984) 2353–2360

ESR and Mössbauer studies of the precipitation process of various ferrites from silicate glasses

T. KOMATSU
Department of Materials Science and Technology, Technological University of Nagaoka, Nagaoka, 949-54 Japan

N. SOGA
Department of Industrial Chemistry, Kyoto University, Kyoto, 606 Japan

ESR and Mössbauer studies of the precipitation process of various ferrites from silicate glasses were made to characterize the precipitation mechanism. The changes in linewidth ($\Delta H_{1/2}$) and effective g-value (g_{eff}) in the ESR spectra of the precipitation process are well explained in terms of super-exchange interaction between magnetic ions and interparticle dipolar interaction between precipitated ferrites. The precipitation tendency of spinel type ferrites from silicate glasses was found to be in the following order: $NiFe_2O_4 \gg CoFe_2O_4 > Fe_3O_4 \geqq ZnFe_2O_4, MnFe_2O_4$. The above order coincided with the order of octahedral site preference energies of divalent transition metal ions.

1. Introduction

Precipitation experiments of various magnetic compounds such as $CoFe_2O_4$, $BaFe_{12}O_{19}$ and YIG from glasses have been carried out by several investigators, not only from technical but also from academic interest [1–5]. Recently, the present authors investigated the $NiFe_2O_4$ precipitation process from silicate glasses in detail using electron spin resonance (ESR) and Mössbauer effect spectroscopy [6–8], and discussed the changes in the magnetic interactions between Fe^{3+} and Ni^{2+} ions, magnetic-order developments, Fe^{3+}–O^{2-} bond characters, Debye temperature of Fe^{3+} ions, and so on. Since then, similar experiments for the precipitation process of other various ferrites from silicate glasses were made to characterize the precipitation mechanism and to obtain information about the relationship between the state of transition metal ions in silicate glasses and the precipitation tendency of ferrites.

In the present paper, the precipitation process of various ferrites (Fe_3O_4, $CoFe_2O_4$, $MnFe_2O_4$, $ZnFe_2O_4$, β-$NaFeO_2$, α-Fe_2O_3 and $SrFe_{12}O_{19}$) from silicate glasses was studied by ESR and Mössbauer effects, and these results are described.

2. Experimental procedure

Sodium silicate glasses of $0.5SiO_2$–$0.3Na_2O$–$x[MO$–$Fe_2O_3]$ system ($x \leqq 0.2$, in mole) were prepared for the study of the precipitation process of spinel type ferrites (MFe_2O_4), where MO is MnO, FeO, CoO and ZnO. The raw materials, SiO_2, Na_2CO_3, MO and Fe_2O_3, all reagent grade, were mixed and melted in an alumina crucible at 1200 to 1400° C for 2 h in an electric furnace (air atmosphere). Then, the molten glass was poured onto a steel plate and pressed quickly to a thickness of about 2 mm. The quenched glasses were heat-treated in an electric furnace (air atmosphere) at various temperatures (350 to 800° C) for 5 h, and then, the heat-treated specimens were quickly removed from the furnace and cooled in air. $0.5SiO_2$–$0.6Na_2O$–$0.4Fe_2O_3$ (precipitated crystals; β-$NaFeO_2$ + α-Fe_2O_3) and $0.469SrO$–$0.286B_2O_3$–$0.245Fe_2O_3$ (precipitated crystals; $SrFe_{12}O_{19}$) glasses were also prepared by the same method. The precipitations of spinel type ferrites and other ferrites were identified by X-ray diffraction analysis using Cu$K\alpha$ radiation, and particularly, the minimum values of x for the precipitations of spinel type ferrites

0022–2461/84 $03.00 + .12

in $0.5SiO_2$–$0.3Na_2O$–x[MO–Fe_2O_3] system were determined.

The ESR measurements for the precipitation process of various ferrites were made using a JES-3BS-X spectrometer operating at X-band frequency ($\nu = 9.3$ GHz) with 100 kHz magnetic field modulation at room temperature. Reference signals of Mn^{2+} ions in MgO were used as the standards for the linewidth $\Delta H_{1/2}$ (peak to peak distance) and effective g-value (g_{eff}). The Mössbauer effect measurements were carried out at room temperature in the quenched as well as heat-treated specimens. For the γ-ray source, 10 mCi ^{57}Co in metallic copper was used. The velocity calibration was obtained from the six-line hyperfine spectra of an iron foil.

3. Results and discussion

3.1. Precipitation process of magnetite, Fe_3O_4

The various glasses of the $0.5SiO_2$–$0.3Na_2O$–x[FeO–Fe_2O_3] system ($x = 0.1$, 0.125, 0.135, 0.15, 0.16, 0.175 and 0.2) were used for ESR and Mössbauer studies of the precipitation process of magnetite, Fe_3O_4. The typical ESR spectrum of a heat-treated specimen and the observed linewidth, $\Delta H_{1/2}$, and effective g-value, g_{eff}, as a function of heat-treatment temperature for the glass of $0.5SiO_2$–$0.3Na_2O$–0.15[FeO–Fe_2O_3] composition are shown in Figs. 1 and 2, respectively. The precipitation of Fe_3O_4 crystals in these silicate glasses was confirmed by X-ray diffraction analysis.

It was found that the $\Delta H_{1/2}$ and g_{eff} change drastically in the Fe_3O_4 precipitation process, as shown in Fig. 2. That is to say, both narrowing and broadening of $\Delta H_{1/2}$ and an increase of g_{eff} were observed. The minimum linewidth ΔH_{min} (290 ± 20 gauss) was obtained in the specimen heat-treated at 560° C for 5 h, and the value of g_{eff} in that specimen was 2.00. It is well known that the super-exchange interactions and dipole–dipole interactions affect the $\Delta H_{1/2}$ and g_{eff} in ESR spectra. Recently, the present authors have discussed the behaviours of $\Delta H_{1/2}$ and g_{eff} in the $NiFe_2O_4$ precipitation process [6]. If the super-exchange coupled pair, Fe^{3+}–O–Fe^{3+}, is formed in the Fe_3O_4 precipitation process, both the exchange narrowed linewidth and the value of $g_{\text{eff}} = 2.00$ would be expected. On the other hand, in ESR spectra of specimens with precipitated Fe_3O_4 crystals, the broad linewidth and large g_{eff} would be observed, because Fe_3O_4 crystal has a large magnetic moment ($4.1\mu_B$). Thus, the narrowing (or $g_{\text{eff}} = 2.00$) and broadening (or large g_{eff}) phenomena in the $\Delta H_{1/2}$ observed in the Fe_3O_4 precipitation process (Fig. 2) may be attributed to the formation of super-exchange coupled pairs (Fe^{3+}–O–Fe^{3+} and Fe^{3+}–O–Fe^{2+}) and the appearance of interparticle dipolar interaction between the precipitated Fe_3O_4 crystals, respectively. The $\Delta H_{1/2}$ and g_{eff} for specimens heat-treated at 650° C for 5 h of various glasses are shown in Fig. 3. As can be seen from Fig. 3, the values of $\Delta H_{1/2}$ and g_{eff} for specimens with precipitated Fe_3O_4 crystals differ appreciably from those for specimens in which no Fe_3O_4 precipitates. This phenomenon proves that the ESR technique is also available to confirm whether Fe_3O_4 crystals have precipitated or not, and the minimum value of x for the precipitation of Fe_3O_4 crystals was determined to be about $x = 0.145$. The Mössbauer spectrum for the Fe_3O_4 precipitated specimen is shown in Fig. 4. It is considered that the observed six hyperfine lines are due to the precipitated Fe_3O_4 crystals.

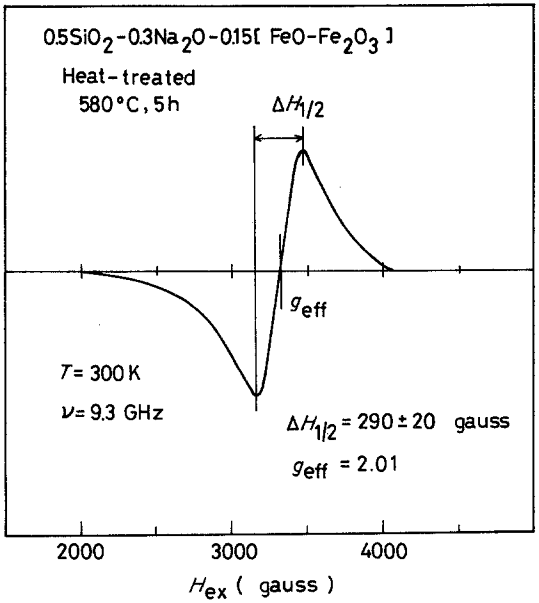

Figure 1 ESR spectrum of heat-treated specimen at 580° C for 5 h of $0.5SiO_2$–$0.3Na_2O$–0.15[FeO–Fe_2O_3] glass.

3.2. Precipitation process of other ferrites

ESR and Mössbauer effect measurements for the precipitation process of other ferrites were made. In Fig. 5, the observed $\Delta H_{1/2}$ and g_{eff} for the heat-treated specimens of $0.5SiO_2$–$0.3Na_2O$–0.165 [ZnO–Fe_2O_3] composition are shown as a function

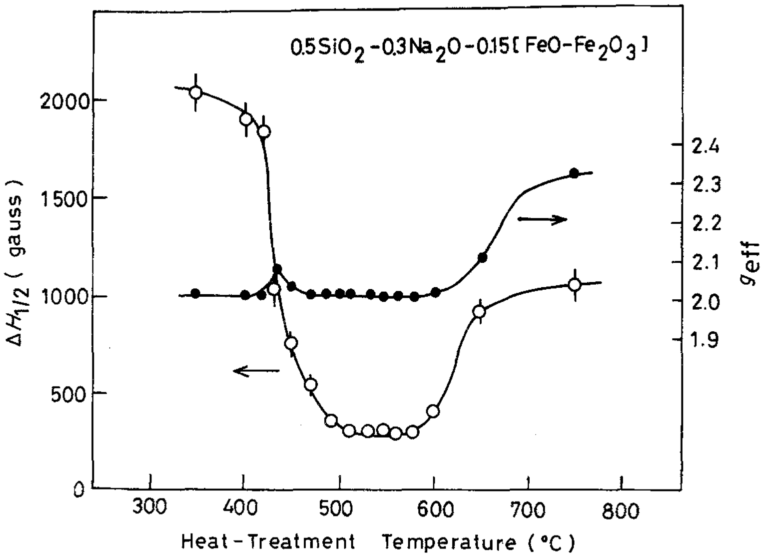

Figure 2 Changes in the linewidth ($\Delta H_{1/2}$) and effective g-value (g_{eff}) in the ESR spectra as a function of heat-treatment temperature for 5 h of $0.5SiO_2-0.3Na_2O-0.15[FeO-Fe_2O_3]$ glass.

of heat-treatment temperature. As can be seen from Fig. 5, a different characteristic feature is observed in $\Delta H_{1/2}$ and g_{eff} in the $ZnFe_2O_4$ precipitation process when compared with the case of the precipitation process of $NiFe_2O_4$ or Fe_3O_4. That is to say, a broadening phenomenon of $\Delta H_{1/2}$ and large g_{eff} were not observed for the $ZnFe_2O_4$ precipitated specimens, while both $\Delta H_{1/2}$ and g_{eff} in the precipitation process of $NiFe_2O_4$ or Fe_3O_4 increased as the precipitation proceeded. These phenomena can be explained by the reason that no interparticle dipolar interaction exists between precipitated $ZnFe_2O_4$ crystals because the magnetic moment of $ZnFe_2O_4$ is zero. The Mössbauer spectrum for the heat-treated specimens of glass of $0.5SiO_2-0.3Na_2O-0.2[ZnO-Fe_2O_3]$ composition is shown in Fig. 6. The spectrum indicates that no other magnetic compounds such as Fe_3O_4 or α-Fe_2O_3 exist.

Cobalt ferrite, $CoFe_2O_4$, also precipitated from the silicate glasses of the $0.5SiO_2-0.3Na_2O-x[CoO-Fe_2O_3]$ system, in which the minimum value of x for the precipitation of $CoFe_2O_4$ crystals was about 0.13. The Mössbauer spectrum for the $CoFe_2O_4$ precipitated specimen is shown in Fig. 6.

So far, it has been shown that the ESR spectra in the precipitation process of spinel type ferrites can be interpreted in terms of super-exchange interaction between magnetic ions and interparticle

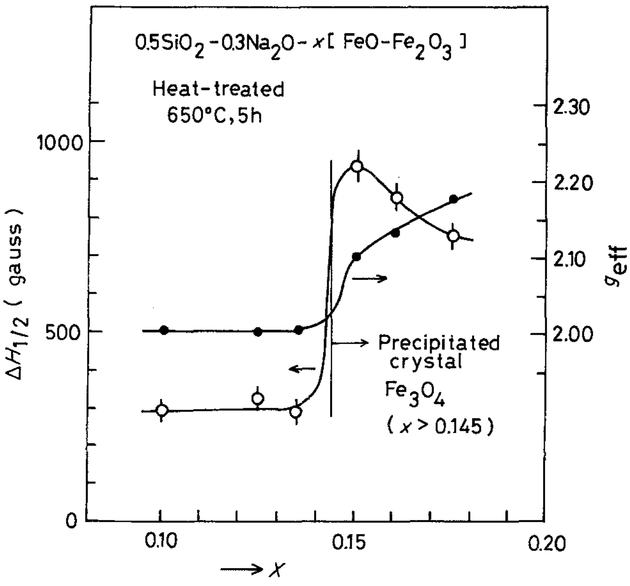

Figure 3 The linewidth ($\Delta H_{1/2}$) and effective g-value (g_{eff}) obtained in the heat-treated specimens at 650° C for 5 h of $0.5SiO_2-0.3Na_2O-x[FeO-Fe_2O_3]$ glasses.

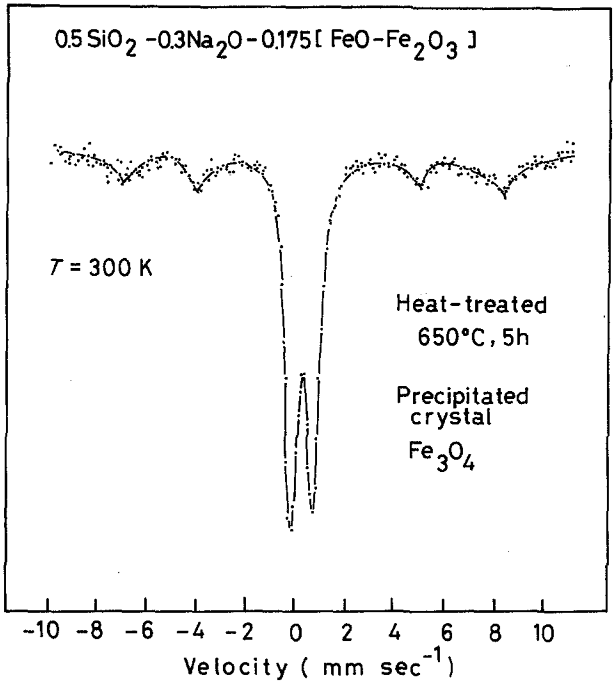

Figure 4 Mössbauer absorption spectrum at 300 K of heat-treated specimen at 650° C for 5 h of $0.5SiO_2$–$0.3Na_2O$–$0.175[FeO$–$Fe_2O_3]$ glass.

dipolar interaction between precipitated ferrites. Thus, in the case of the precipitation process of magnetic compounds which show a very strong super-exchange interaction between magnetic ions and have no magnetic moment (i.e. no interparticle dipolar interaction), a very narrowed linewidth would be obtained in the precipitation process. Conversely, the linewidth of the ESR spectrum for the precipitated specimen of magnetic compounds which have a large magnetic moment would be very broad. As the former case, the precipitation process of haematite, α-Fe_2O_3, and sodium ferrite, β-$NaFeO_2$, from silicate glass was studied. As the latter case, the precipitation process of strontium ferrite, $SrFe_{12}O_{19}$, from a borate glass was investigated. As shown in Table I, both α-Fe_2O_3 and β-$NaFeO_2$ crystals show weak ferromagnetism arising from the presence of a Dzyaloshinsky type interaction, and have high Curie temperatures and very small magnetic moments, while the $SrFe_{12}O_{19}$ crystal has an extremely large magnetic moment. Previously, experiments on the precipitations of α-Fe_2O_3 and β-$NaFeO_2$ from silicate glasses and $SrFe_{12}O_{19}$ from borate glasses have been reported by Collins and Mulay [9] and Goto and Takahashi [10], respectively.

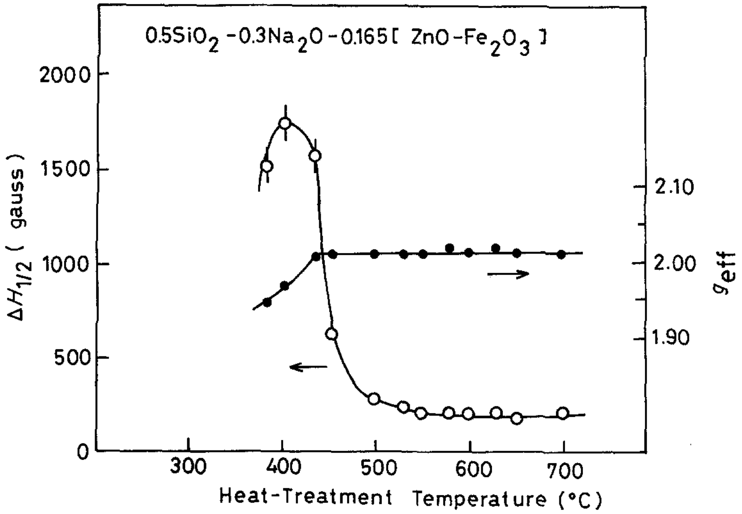

Figure 5 Changes in the linewidth ($\Delta H_{1/2}$) and effective g-value (g_{eff}) in the ESR spectra as a function of heat-treatment temperature for 5 h of $0.5SiO_2$–$0.3Na_2O$–$0.165[ZnO$–$Fe_2O_3]$ glass.

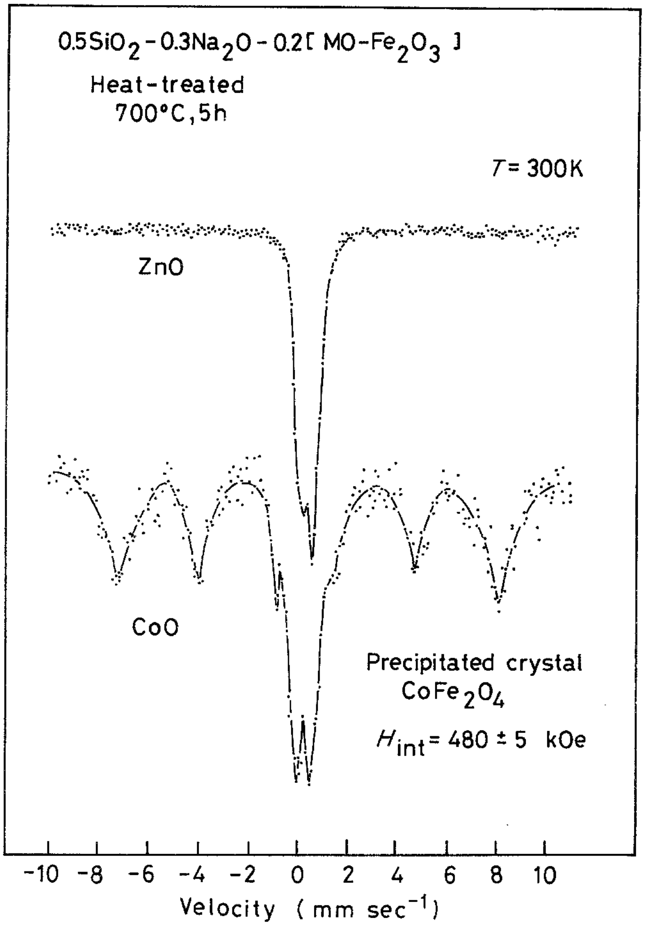

Figure 6 Mössbauer absorption spectra at 300 K for heat-treated specimens at 700° C for 5 h of silicate glasses containing ZnO or CoO.

The precipitation of α-Fe_2O_3 and β-$NaFeO_2$ crystals was obtained from $0.5SiO_2$–$0.6Na_2O$–$0.4Fe_2O_3$ glass by the heat-treatment. The extremely narrowed linewidth, $\Delta H_{1/2}$, and the value of $g_{eff} = 2.00$ were obtained in the precipitation process of these crystals and the values are summarized in Table II. A typical ESR spectrum for a heat-treatment specimen is shown in Fig. 7. The observed values of $\Delta H_{1/2}$ in the $SrFe_{12}O_{19}$ precipitation process from $0.469SrO$–$0.286B_2O_3$–$0.245Fe_2O_3$ glass are summarized in Table III. The $\Delta H_{1/2}$ becomes extremely broad as the $SrFe_{12}O_{19}$ precipitation proceeds. These results agree well with the above prediction.

3.3. Exchange narrowed linewidth

In the precipitation process of ferrites from silicate glasses, the exchange narrowed linewidth arising from the formation of super-exchange coupled pairs between magnetic ions is observed in the

TABLE I Magnetic properties of various ferrites

Material	Spin configuration	Curie temp. T_C or Néel temp. T_N (K)	Magnetic moment (μ_B)
$NiFe_2O_4$	ferrimagnetism	863	2.2
$MnFe_2O_4$	ferrimagnetism	573	4.6
$FeFe_2O_4$	ferrimagnetism	863	4.1
$CoFe_2O_4$	ferrimagnetism	793	3.9
$ZnFe_2O_4$	antiferromagnetism	9.5	0
α-Fe_2O_3	weak ferromagnetism	953	0.03
β-$NaFeO_2$	weak ferromagnetism	723	
$SrFe_{12}O_{19}$	ferrimagnetism	733	20.6

TABLE II ESR parameters at 300 K for the quenched and heat-treated specimens of the $0.5SiO_2$–$0.6Na_2O$–$0.4Fe_2O_3$ glass

Specimen	$\Delta H_{1/2}$ (gauss)	g_{eff}
Quenched*	125 ± 10	2.01
Heat-treated		
600° C, 5 h	75 ± 10	2.00
700° C, 5 h	50 ± 10	2.00
800° C, 5 h	60 ± 10	2.00

*Somewhat devitrified.

TABLE III ESR parameter* at 300 K for the heat-treated specimens of the $0.469SrO$–$0.286B_2O_3$–$0.245Fe_2O_3$ glass

Specimen	$\Delta H_{1/2}$ (gauss)
Heat-treated	
600° C, 5 h	850 ± 50
650° C, 5 h	1300 ± 100
700° C, 5 h	1700 ± 100

*ESR spectra were asymmetrical, thus g_{eff} was not determined.

ESR experiment. The stronger the super-exchange coupled pairs formed in the precipitation process are, the narrower the linewidth. In the initial stage of the precipitation process, it is a very interesting and important problem how strong super-exchange interactions are formed. The minimum linewidth, ΔH_{min}, observed in the precipitation process of various ferrites from silicate glasses is shown in Fig. 8.

As can be seen from Fig. 8, the ΔH_{min} observed in the precipitation process of ferrites is narrower in comparison with the ΔH_{min} observed in the crystallization process of $5Na_2O \cdot Fe_2O_3 \cdot 8SiO_2$, which is a paramagnetic compound [11]. The narrowest linewidth is observed in the precipitation process of α-Fe_2O_3 and β-$NaFeO_2$. As described in the previous section, no interparticle dipolar interaction appears in the precipitation process of these compounds. In other words, the narrowest linewidth would arise from the formation of long-range ordering of the super-exchange coupled Fe^{3+}–O–Fe^{3+} pair. Among the precipitation processes of $NiFe_2O_4$, Fe_3O_4 and $ZnFe_2O_4$, the linewidth for the case of the $NiFe_2O_4$ precipitation process was narrowest. This means that the super-exchange coupled Fe^{3+}–O–Ni^{2+} pair formed in the $NiFe_2O_4$ precipitation process is stronger than the super-exchange coupled Fe^{3+}–O–Fe^{3+} or Fe^{3+}–O–Fe^{2+} pair formed in the precipitation process of Fe_3O_4 and $ZnFe_2O_4$.

3.4. Precipitation tendency of ferrites

From the comparison of the data of ESR, Mössbauer effect and X-ray diffraction analysis described above, the precipitation tendency of spinel type ferrites MFe_2O_4 from sodium silicate glasses of the $0.5SiO_2$–$0.3Na_2O$–x[MO–Fe_2O_3] system was found to be in the following order:

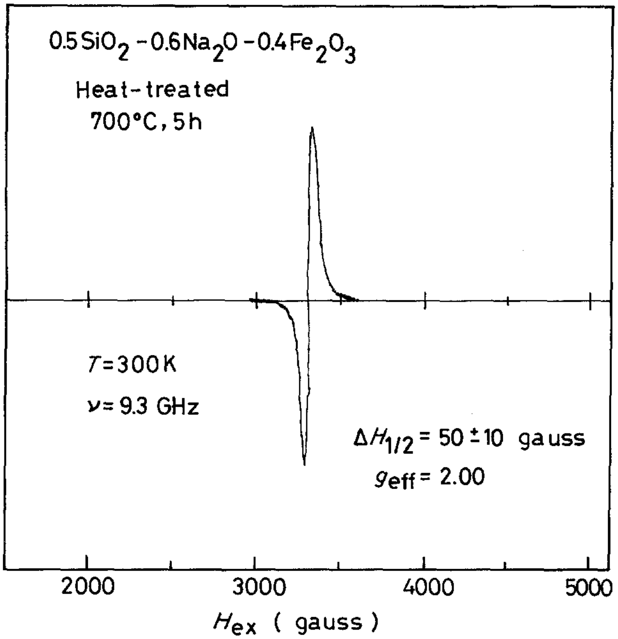

Figure 7 ESR spectrum of heat-treated specimen at 700° C for 5 h of $0.5SiO_2$–$0.6Na_2O$–$0.4Fe_2O_3$ glass.

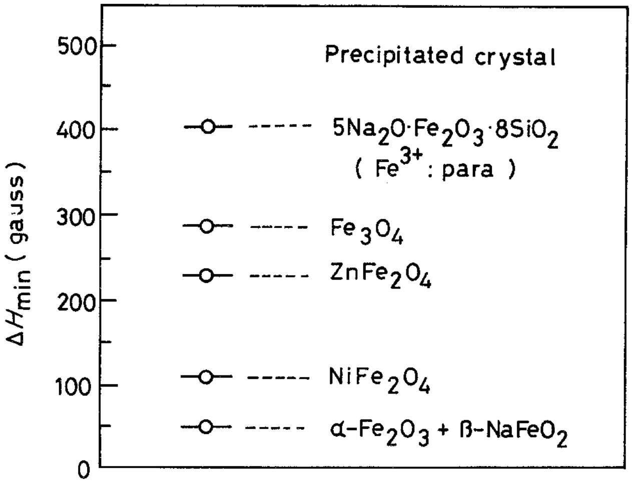

Figure 8 The minimum linewidth (ΔH_{min}) in ESR spectra obtained in the precipitation process of various ferrites from silicate glasses.

$$NiFe_2O_4 \gg CoFe_2O_4 > Fe_3O_4 \geqq ZnFe_2O_4, MnFe_2O_4$$

It is of particular interest to determine what parameter governs the precipitation tendency of MFe_2O_4 crystals from silicate glasses.

To compare the state of Fe^{3+} ions in quenched glasses containing different divalent transition metal ions, Mössbauer effect measurements of various quenched glasses of $0.5SiO_2$–$0.3Na_2O$–$0.1[MO$–$Fe_2O_3]$ composition were made. The obtained values of isomer shift (I.S.) and quadrupole splitting (ΔE) are summarized in Table IV. As can be seen from Table IV, the isomer shift and quadrupole splitting are almost the same, and this means that in the various silicate glasses containing different divalent transition metal ions, the nature of the Fe^{3+}–O^{2-} bond and the site symmetry of Fe^{3+} ions are not so much different. Consequently, it may be reasonable to consider that the difference of the precipitation tendency of spinel type ferrites MFe_2O_4 from sodium silicate glasses arises from the difference in the state and behaviour of divalent transition metal ions in silicate glasses.

TABLE IV Isomer shift (I.S.) and quadrupole splitting (ΔE) for Fe^{3+} ions at 300 K in quenched glasses of $0.5SiO_2$–$0.3Na_2O$–$0.1[MO$–$Fe_2O_3]$ system

MO	I.S. ($mm\,sec^{-1}$)	ΔE ($mm\,sec^{-1}$)
MnO	0.25 ± 0.02	0.84 ± 0.03
FeO*	0.23 ± 0.02	0.79 ± 0.03
CoO	0.24 ± 0.02	0.88 ± 0.03
NiO	0.25 ± 0.02	0.84 ± 0.03
ZnO	0.24 ± 0.02	0.86 ± 0.03

*The glass was prepared in air atmosphere, thus Fe^{2+} ions were oxidized somewhat to Fe^{3+} ions.

Kruchinin and Pogodina [12] have reported that the influence of transition metal oxides (catalysts) on the crystallization tendency of glasses to fine-grained products increases in the series MnO → FeO → CoO → NiO. In the field of geology, the state and behaviour of transition metal ions in magma (silicate system) have been extensively investigated. Williams [13] has reported the order of uptake of trace amounts of transition metal ions in minerals to be $Ni^{2+} > Co^{2+} > Fe^{2+} > Mn^{2+} \geqq Zn^{2+}$ and has correlated the above order with the order of crystal-field stabilization energies of transition metal ions in octahedral sites. The importance of crystal-field effects for the state and behaviour of transition metal ions in silicate systems has been pointed out by several investigators [14–17]. Particularly, on the above order, Burns and Fyfe [16] have concluded that, because of added stability, it is energetically more favourable for these ions to be removed from tetrahedral coordination in a magma and to enter into octahedral sites in minerals when crystallized from the magma.

The precipitation tendency of MFe_2O_4 crystals from silicate glasses agrees well with the order of octahedral site preference energy of divalent transition metal ions, as in the case of the behaviour of transition metal ions in a magma–mineral system. The crystal structures of $NiFe_2O_4$, $CoFe_2O_4$ and Fe_3O_4 are inverse spinel, while $ZnFe_2O_4$ crystal is normal spinel. Thus, Ni^{2+}, Co^{2+} and Fe^{2+} ions occupy the octahedral sites and Zn^{2+} ions occupy tetrahedral sites. On the other hand, $MnFe_2O_4$ crystal is partly inverse spinel, and Mn^{2+} ions occupy both octahedral (20%) and tetrahedral (80%) sites. $NiFe_2O_4$ crystals precipitate easily from silicate glasses. An Ni^{2+} ion has a large octahedral site preference energy of 20.6 kcal mol^{-1} compared with other transition metal ions [18] and generally occupies a symmetrical octahedral site in many minerals as well as $NiFe_2O_4$ crystal. In other words, an Ni^{2+} is energetically unsatisfied in tetrahedral or distorted octahedral environments. Burns and Fyfe [14] have reported, using optical absorption spectra, that an Ni^{2+} ion occupies both octahedral and tetrahedral sites in sodium silicate glasses. It is well known that alkali silicate liquids produce a large array of tetrahedral coordinate sites. Furthermore, the Mössbauer effect measurements for Fe^{3+} ions in sodium silicate glasses show that the octahedral sites in sodium silicate glasses are distorted largely. Therefore, in the glassy state, Ni^{2+} ions may take such tetrahedral or distorted octahedral sites in sodium silicate glasses. During the precipitation process, however, Ni^{2+} ions should enter energetically into the undistorted octahedral sites available in the growing $NiFe_2O_4$ crystals rather than remaining in glasses. This information is considered quite useful in designing the devitrification method for making ferrites from glasses.

4. Summary

Various ferrites precipitate from sodium silicate glasses and the precipitation process was studied by ESR and Mössbauer effect measurements. The linewidth and effective g-value in ESR spectra are well explained in terms of super-exchange interaction between magnetic ions and interparticle dipolar interaction between precipitated ferrites. The precipitation tendency of spinel type ferrites agrees with the order of octahedral site preference energies of divalent transition metal ions.

Acknowledgements

The authors would like to thank Dr Y. Isozumi, Kyoto University, for helpful discussion and the Mössbauer effect measurements.

References

1. R. R. SHAW and J. H. HEASLEY, *J. Amer. Ceram. Soc.* 50 (1967) 297.
2. W. J. S. BLACKBURN and B. P. TILLEY, *J. Mater. Sci.* 9 (1974) 1265.
3. B. T. SHIRK and W. R. BUESSEM, *J. Amer. Ceram. Soc.* 53 (1970) 192.
4. M. O'HORO and R. STEINITZ, *Mater. Res. Bull.* 3 (1968) 117.
5. A. PRASAD, D. BAHADUR, R. M. SINGRU and D. CHAKRAVORTY, *J. Mater. Sci.* 17 (1982) 2687.
6. T. KOMATSU, N. SOGA and M. KUNUGI, *J. Appl. Phys.* 50 (1979) 6469.
7. T. KOMATSU and N. SOGA, *ibid.* **51** (1980) 601.
8. *Idem, ibid.* **51** (1980) 5926.
9. D. W. COLLINS and L. N. MULAY, *J. Amer. Ceram. Soc.* 53 (1970) 74.
10. Y. GOTO and K. TAKAHASHI, *J. Ceram. Assoc. Jpn.* 80 (1972) 358.
11. T. KOMATSU and N. SOGA, *J. Chem. Phys.* 72 (1980) 1781.
12. Yu. D. KRUCHININ and T. M. POGODINA, *J. Appl. Chem. USSR,* Consultants Bur. Tranl. **45** (1972) 1500.
13. R. J. P. WILLIAMS, *Nature* **184** (1959) 44.
14. R. G. BURNS and W. S. FYFE, *Chem. Geol.* **1** (1966) 49.
15. C. D. CURTIS, *Geochim. Cosmochim. Acta* **28** (1964) 389.
16. R. G. BURNS and W. S. FYFE, *Science* **144** (1964) 1001.
17. T. M. SEWARD, *Chem. Geol.* 7 (1971) 73.
18. J. D. DUNITZ and L. E. ORGEL, *J. Phys. Chem. Solids* 3 (1957) 318.

Received 14 July
and accepted 4 October 1983